Available online at www.sciencedirect.com

ScienceDirect

journal homepage: www.JournalofSurgicalResearch.com

Enhanced vascular regeneration with chemically/physically treated bovine/human pericardium in rodent

Mathieu van Steenberghe, MD, MSc,[a,*] *Thomas Schubert, MD, PhD,*[a,b] *Daela Xhema, BSc,*[a] *Caroline Bouzin, PhD,*[c] *Yves Guiot, PhD,*[d] *Jérôme Duisit, DDS, MD,*[a] *Karim Abdelhamid, MD,*[e] *and Pierre Gianello, MD, PhD*[a]

[a] *Université catholique de Louvain (UCL), Secteur des Sciences de la Santé, Institut de Recherche expérimentale et clinique (IREC), Pôle de Chirurgie expérimentale et Transplantation (CHEX), Brussels, Belgium*

[b] *Cliniques Universitaires Saint-Luc, Service d'orthopédie et de traumatologie de l'appareil locomoteur, Brussels, Belgium*

[c] *Université catholique de Louvain, IREC Imaging Platform (2IP), Institut de Recherche expérimentale et clinique (IREC), Brussels, Belgium*

[d] *Cliniques universitaires Saint-Luc, Service d'anatomopathologie, Brussels, Belgium*

[e] *Centre Hospitalier Universitaire Vaudois, polyclinique médicale universitaire, Lausanne, Switzerland*

ARTICLE INFO

Article history:
Received 20 June 2017
Received in revised form
23 August 2017
Accepted 29 September 2017
Available online xxx

Keywords:
Decellularization
Cardiovascular tissue engineering
Biocompatibility
Bovine/human pericardium
Regeneration

ABSTRACT

Background: Glutaraldehyde-treated pericardia for cardiovascular applications have poor long-term clinical results. The efficacy of a combined physical/chemical treatment to improve pericardium biocompatibility and vascular regeneration was assessed and compared with detergent treatment and two commercial bovine pericardia: PeriGuard (DGBP) and Edwards pericardium (nDGBP). The physical and chemical process was applied to bovine and human pericardia (DBP-DHP), and the detergent process was applied to bovine (DDBP).

Material and methods: Native (NBP) and treated bovine tissues were assessed for decellularization (HE/DAPI/DNA/α-Gal and MHC-1 staining) and mechanical integrity *ex vivo*. Twenty Wistar rats received subcutaneous patches of each bovine tissue to assess immunogenic response up to 4 months (flow cytometry). Ten additional rats received four subcutaneous bovine-treated patches (one/condition) to evaluate the inflammatory reaction (CD3/CD68 immunostaining), calcification (von Kossa staining/calcium quantification), and integration assessment (Hematoxylin and eosin staining). Finally, 15 rodents received a patch on the aorta (DBP $n = 5$, DHP $n = 5$, and DGBP $n = 5$), and vascular biocompatibility and arterial wall regeneration were assessed after 4 months (CD3/CD68/CD31/ASMA and Miller staining).

Results: DBP reached the higher level of decellularization, no immunogenic response whereas maintaining mechanical properties. DBP induced the lowest level grade of inflammation after 2 months ($P < 0.05$) concomitantly for better remodeling. No complications occurred with DBP and DHP where vascular regeneration was confirmed. Moreover, they induced a low level of CD3/CD68 infiltrations.

* *Corresponding author*. Université catholique de Louvain, Pôle de chirurgie expérimentale et transplantation, Avenue Hippocrate 55, Bte B1.55.04, B-1200 Brussels, Belgium. Tel.: +32 (0)2 764 55 86; fax: +32 (0)2 764 55 89.
E-mail address: mathieu.vansteenberghe@uclouvain.be (M. van Steenberghe).

https://doi.org/10.1016/j.jss.2017.09.043

Conclusions: This process significantly reduces immunogenicity and improves biocompatibility of bovine and human pericardia for better vascular regeneration.

Introduction

Bovine and human pericardia (BP-HP) are largely used in cardiovascular surgery to repair valves or congenital heart defects and for a large spectrum of other reconstructive procedures.

The standard treatment of pericardium for clinical use is glutaraldehyde fixation (G)[1] to produce cross-links in the cellular and extracellular matrix (ECM) improving mechanical resistance and to reduce graft immunogenicity, especially for xenogeneic tissue. Aldehyde treatment is, however, also cytotoxic and does not completely suppress the immunological reaction against xenogeneic graft.[2] In fact, the G-treatment leaves dead cells/cell debris in the tissue and does not completely remove phospholipids, thereby leading to chronic inflammation and calcification of grafted tissues.[3] The consequences are subsequent function and structural deterioration of prostheses.[4] This deterioration occurs earlier in younger patients because of their strong immunity and high phosphocalcic metabolism.[5]

Decellularization was therefore proposed to improve long-term efficacy of these prostheses. It enhances *in situ* graft biocompatibility and improves recellularization toward host-tissue regeneration with similar native properties. The tissue decellularization process must remove cells/antigens and preserve extracellular matrix and mechanical properties. Different decellularization treatments have been used, and the most popular are those using detergents and/or enzymes.[6] New products (ECM) based on those protocols are already commercialized for cardiovascular applications. However, short-term results with some of those implants in clinical practice did not demonstrate convincing results in the pediatric population.[7] Better results regarding the absence of calcification and/or aneurysm formation were achieved at a short follow-up with some others for pediatric cardiac reconstructions.[8,9]

We recently studied a tissue process based on non-detergent methods on different xeno/allogeneic tissues and, in particular, on human pericardium that can be banked and proposed as a decellularized homograft.[10,11] Our *in vitro* and *in vivo* results in a rodent vascular model showed that this decellularization method offers excellent short-term results in terms of biocompatibility. Moreover, our processed implants and more precisely the human pericardium demonstrated significantly better results in terms of biocompatibility when compared to a conventional glutaraldehyde-fixed pericardium.[11]

Since the availability of human pericardium is limited, the source of xenogeneic tissue must be considered as an alternative although it carries noncellular xenogeneic antigens responsible for higher immunogenic host response, and it is difficult to remove without ECM damage.[12,13]

Therefore, the present study compared the *in vitro* and *in vivo* (subcutaneous), the efficacy of a physical, chemical nondetergent/enzymatic and glutaraldehyde-free process to decellularize and improve the biocompatibility of bovine pericardium (DBP) with (1) a conventional detergent/glutaraldehyde-free process (DDBP) as well as with two commercially treated available bovine pericardia currently used in clinical setup, (2) the supple PeriGuard bovine pericardium (DGBP) similarly treated as DBP, and (3) the Edwards Lifesciences bovine pericardium (nDGBP), which is not decellularized and is considered a standard in cardiovascular surgery.

In vitro studies compared these tissues with native tissue regarding cellularity (HE-DAPI), DNA content, antigenicity (MHC-class I and Gal1,3-Galβ1,4GlcNAc-R [α-Gal] antigens immunostaining), and biomechanical properties (elongation stress test).

In vivo, the rodent systemic immune response, local inflammatory reaction, remodeling of the implant, and calcification occurrences were assessed after subcutaneous implantation and compared between each bovine pericardium tissue conditions.

In a supplementary *in vivo* model, a vascular patch was achieved on rat aorta: both DBP and DHP treated by combined physical/chemical decellularization process were compared with the PeriGuard (DGBP) regarding vascular biocompatibility and vascular regeneration after 4 months of follow-up.

Material and methods

Sources of matrices

Bovine pericardium (BP) was procured from a local slaughterhouse (Eurovlees, Zele, Belgium). Human pericardium (HP) was procured according to the common standards of the European Association of Musculoskeletal Transplantation (EAMST, Vienna, 1997). Human pericardium was harvested in agreement with the Ethic Committee of the Université catholique de Louvain.

The tissues were rinsed with sterile ringer solution, mechanically stripped of loose adipose tissue and frozen at −80°C.

The two commercialized pericardia purchased were the following: Edwards Lifesciences bovine pericardium (Edwards Lifesciences Corporation, Irvine, CA), nondecellularized and preserved in glutaraldehyde (nDGBP) and Supple PeriGuard bovine pericardium (Baxter International, Inc, Deerfield, IL), treated with NaOH 1N before glutaraldehyde preservation (DGBP).

Matrix preparation

Before processing, tissues were thawed and washed in sterile ringer solution.

The pericardium was cut into pieces of 15 cm by 10 cm. Two treatment protocols were conducted. One process was

based on a conventional detergent protocol previously published: bovine pericardial pieces were incubated for 48 hours in an aqueous solution containing 0.5% sodium deoxycholate (SDC) and 0.5% sodium dodecylsulfate (SDS) under continuous agitation followed by a 72-hour rinsing step in a continuous flow of demineralized water.[14]

As previously described, the second process consists of a succession of baths of acetone, ethanol, NaOH, and H_2O_2. This chemical treatment ensures defatting, prions/viruses, and bacterial inactivation.[11]

Finally, the ECM was frozen at −80°C, individually packed and sterilized by gamma irradiation (25 KGy). The tissues collected were respectively named detergent decellularized bovine pericardium (DDBP), decellularized bovine/human pericardium (DBP-DHP) for tissues treated with the second process.

In vitro *prosthesis characterization*

Human pericardium was previously characterized.[11] The *in vitro* tests in this study were conducted on bovine pericardial tissues.

Hematoxylin and eosin/DAPI staining
Decellularization was evaluated first by hemalun eosin and 40.6-diamidino-2-phenylindole (DAPI; 1 μg/ml) staining (Abbot Molecular Inc) on four paraformaldehyde-(4%) fixed slices from four different tissues of the five bovine tissues types (NBP, nDGBP, DGBP, DBP, and DDBP) as previously described.[11] From each sample, five sections were photographed at high definition under structured illumination using a Zeiss AxioImager-Apotome system. Nuclei were counted using imageJ (NIH, open source).

Antigen removal
The presence of residual antigens such as α-Gal and MHC I was investigated by immunohistochemistry as previously described.[11]

DNA quantification
DNA was extracted with DNeasy Blood & Tissue Kit (QIAamp DNA Mini Kit, QIAGEN, Hilden, Germany). Four tissues per condition were used, and two samples per tissue were processed. The extracted DNA was quantified with the Quant-it Picrogreen DNA assay kit (Invitrogen, CA), according to manufacturers' protocol. Fluorescence was read at 480 nm and 520 nm. Final DNA concentration was expressed in ng/mg dry weight.

Scanning electron microscopy
Tissue samples from each tissue condition were observed with a field emission scanning electron microscope (JSM-7600F, JEOL). Tissues were fixed with 2.5% glutaraldehyde overnight at 4°C. Samples were then washed with phosphate-buffered saline (GIBCO Life Technologies, Diegem, Belgium) and were gradually dehydrated by successive immersion in increasing concentrations of ethanol for 15 min each. Before scanning electron microscopy (SEM) imaging, tissues were critical point dried and coated with an 8-nm layer of gold. SEM measurements were performed at 15 keV.

Mechanical properties
Uniaxial mechanical resistance tests were performed on four samples of four tissues per condition except for commercially available tissues DGP and nDGP with four samples in one tissue. Mechanical testing was performed as previously described using an Instron traction system with Instron bluehill software (Model 5600, Instron, Canton, MA).[11] The structural properties of the matrices were represented by stiffness (Newton/mm) and ultimate load (Newton). These parameters were compared between native and processed pericardium.

In vivo study

Surgical procedures

Animals were housed according to the guidelines of the Belgian Ministry of Agriculture and Animal Care. All procedures were approved by the local Ethics Committee for Animal Care of the Université Catholique de Louvain.

Subcutaneous implantation
Two series of experiments were conducted. In the first series, 10 male or female 160-200 g Wistar rats received one patch (1 × 1.5 cm), from each treated bovine pericardium condition (nDGBP, DGBP, DDBP, and DBP) in the subcutaneous abdominal space under general anesthesia (zoletil, xylazine, and ketamine mix) to assess their biocompatibility. After 2 and 4 months, five rats were euthanized with intracardiac injection of T61. The pericardial patches were collected, rinsed in sterile phosphate-buffered saline, and divided in two parts for histologic analysis and calcium quantification.

In the second series, 20 male or female 160-200 g Wistar rats were randomly assigned into nDGBP, DGBP, DDBP, DBP, and native bovine pericardium (NBP) groups with each group consisting of four animals to assess immunogenicity of the tissues. NBP served as positive control. One patch was implanted subcutaneously under abdominal skin after general anesthesia. The serum of each animal was collected before implantation, after 1 month and 4 months, for estimating antibody response against bovine pericardial antigens.

Intravascular implantation
Fifteen male or female 200 g Wistar rats received a patch (1 × 0.5 cm) on the abdominal aorta as previously described.[11] There were three groups of five rats divided as follows: DBP, DHP, and DGBP. The rats were followed up for 4 months. No antiaggregation or anticoagulation was performed during follow-up. After 4 months, the rats were euthanized. The patched aorta was harvested, rinsed with saline serum fixed overnight in 4% formaldehyde and paraffin embedded.

Histological evaluation

Coloration and staining
Serial sections (5 μm thickness) of paraffin-embedded tissues were mounted on glass and dried for 12 hours at 37°C.

Hematoxylin and eosin and von Kossa staining assessed ECM remodeling/cell infiltration and ECM calcification,

respectively, in two models. Miller staining was performed to assess elastic fibers regeneration in the vascular model. Slides were digitalized at a 20× magnification with a SCN400 slide scanner (Leica, Wetzlar, Germany) and visualized on the Digital Image Hub (Leica Biosystems, Dublin, Ireland).

Inflammatory reaction was assessed with CD3 and CD68 immunostaining in subcutaneous and intravascular models. Immunostaining for alpha-smooth muscle actin (ASMA) and CD31 were conducted in the vascular model for arterial wall regeneration investigation. After manual deparaffinization, endogenous peroxidases were inhibited for 20 minutes with 3% hydrogen peroxide in methanol. Then, 5 μm sections were subjected to antigen retrieval in 10-mM citrate buffer of pH 5.7 and then to specific antigen binding sites blocking (Tris buffered saline solution containing 5% Bovine serum albumine and 0.05% Triton). Rabbit anti ASMA (polyclonal, Abcam ab5694, 1/300 dilution), rabbit anti-CD3 (polyclonal, Abcam ab828, 1/50 dilution), or mouse anti-CD68 (clone ED1, Abcam ab31630, 1/600 dilution) primary antibodies were incubated overnight at 4°C in Tris buffered saline containing 1% Bovine serum albumine and 0.05% Triton. This was followed by an incubation with envision anti-rabbit antibodies (Dako K4003), envision anti-mouse antibodies (Dako K4001), or with an anti-mouse (Jackson Immunoresearch 115-035-062) secondary antibody for 30 minutes at room temperature. This reaction was visualized using DAB (Dako K3468). After counterstaining with hematoxylin, slides were dehydrated and cover slipped. The slides were finally digitalized and visualized on the Digital Image Hub.

For immunofluorescent costaining, the same protocol was applied using mouse anti-ASMA (Dako M0851, 1/100 dilution) and rabbit anti-CD31 (Abcam ab28364, 1/50 dilution) primary antibodies and AlexaFluor568 anti-rabbit and AlexaFluor647 anti-mouse secondary antibodies (Life Technologies) incubated at a 1/1000 dilution for 1 hour at room temperature. Nuclei were stained with DAPI, and labeled sections were imaged by epifluorescence with a 2.5× N-Achroplan objective or by structured illumination with a 20× Plan-Apochromat objective using a Zeiss AxioImager microscope equipped with an ApoTome module.

Morphometry

In the subcutaneous model, five regions of interest (ROI) at the junction of the patch and surrounding tissues were analyzed at 20 × magnification with a grid representing a surface of 0.12 mm^2. In the rodent vascular model, the counts were done in the external portion of the reconstructed wall where the inflammatory reaction occurs, at20 × magnification with a grid representing a surface of 0.12 mm^2 as previously described.[11]

The thickness of the new media was measured on Hematoxylin and eosin slides for each tissue for each experiment at 4 months with Digital Image Hub (Leica Biosystems, Dublin, Ireland). The media of the native aorta was measured on the same slide. Three measures were done for the new media: two externals, one central to the patch, and three for the opposite native media. The new media mean thickness for reconstructed portion was calculated for each tissue (DGBP-DBP and DHP). Those thicknesses were compared between them and with mean thickness of contralateral native media.

Calcium analysis

Harvested tissue samples were washed with normal saline, dried at 70°C for 24 hours, and weighed. Samples were then hydrolyzed with 1.0 N HCl solution. The calcium content of the hydrolysate was measured calorimetrically with the O-cresolphthalein complexone method (Calcium Colorimetric Assay Kit, Sigma-Aldrich, Diegem, Belgium) as previously described[15] using an automatic chemistry analyzer (Bio rad, Belgium). Calcium contents were expressed as μg mg−1 dry weight.

Immunogenicity/systemic antibody response

Isolation of peripheral blood mononuclear cells (PBMCS)

Freshly drawn, heparinized whole bovine blood procured from UCL farm (Centre Alphonse de Marbaix, Corroy le Grand, Belgium) was diluted with Hanks' buffered saline solution (HBSS) (GIBCO Life Technologies), and the mononuclear cells were obtained with gradient centrifugation (2500 rpm, 20 min, room temperature) using lymphocyte separation medium (Ficoll-Paque Plus, GE Healthcare Life Sciences, Diegem, Belgium). Mononuclear cells were washed twice with HBSS. Freshly isolated peripheral blood mononuclear cells (PBMCs) were assayed for flow cytometry.

Detection of antidonor alloantibody (IgG) by flow cytometry

PBMCs (250,000 cells) were incubated with recipient sera for 30 min at room temperature. Before the incubation, the sera were decomplemented for 30 min at 56°C. After washing with fluorescence-activated cell sorting buffers (HBSS containing 0.5% fetal bovine serum and 0.1% sodium azide), saturating amounts of 5 μg/ml fluorescein isothiocyanate–conjugated (FITC) mouse anti-rat IgG monoclonal antibody MARK-1 (Synabs Company, Bruxelles, Belgium) were added and incubated for 30 min at room temperature and then washed twice. Each analysis included the appropriate fluorescein isothiocyanate–conjugated antibody with only PBMCs, for nonspecific reaction. For a positive control group of immunizations, we were considering the native pericardium group. Cells were acquired and analyzed with BD FACS Calibur (BD Bioscience Benelux NV, Erembodegem, Belgium) driven by CellQuest Pro software (BD Bioscience). We tested the sera with the receiver PBMC to show that the positivity was correlated with the immunization.

A positive reaction was defined as a shift of more than 10 channels in mean fluorescence intensity when testing donor lymphocytes with posttransplantation (day 30) sera and comparing mean fluorescence intensity with pretransplant serum (day 0).

Statistical analysis

One-sample Kolmogorov-Smirnov tests and QQ-plots were used to ensure the normal distribution of values. Results were expressed as means ± standard deviation or in ratios. The statistical significance of differences between experimental groups was tested by Student *t*-test or one-way analysis of variance with a Bonferroni's post hoc test. The statistical tests were carried out with PASW 18. Differences were considered to be significant at $P < 0.05$.

Results

In vitro

Decellularization

The hematoxylin and eosin staining confirmed the decellularization of DBP and DDBP when nDGBP and NBP appeared normally cellularized (Fig. 1A/E/M/Q). Some nuclei from endothelial cells of peripheral vascular structures were, however, detected in the depth of DGBP (Fig. 1I).

The DAPI staining showed the absence of fluorescence for DBP, DGBP, and some signals for DDBP (0.0 ± 1.33 *versus* 0.0 ± 0.0 *versus* 37 ± 71.86 positive cells/mm^2 with $P > 0.05$) (Fig. 1R/J/N/U). The highest counts were for NBP and nDGBP in comparison to other tissues (1073.88 ± 317.15 cells/mm^2 and 624.02 ± 80.69 cells/mm^2 with $P < 0.05$; Fig. 1U).

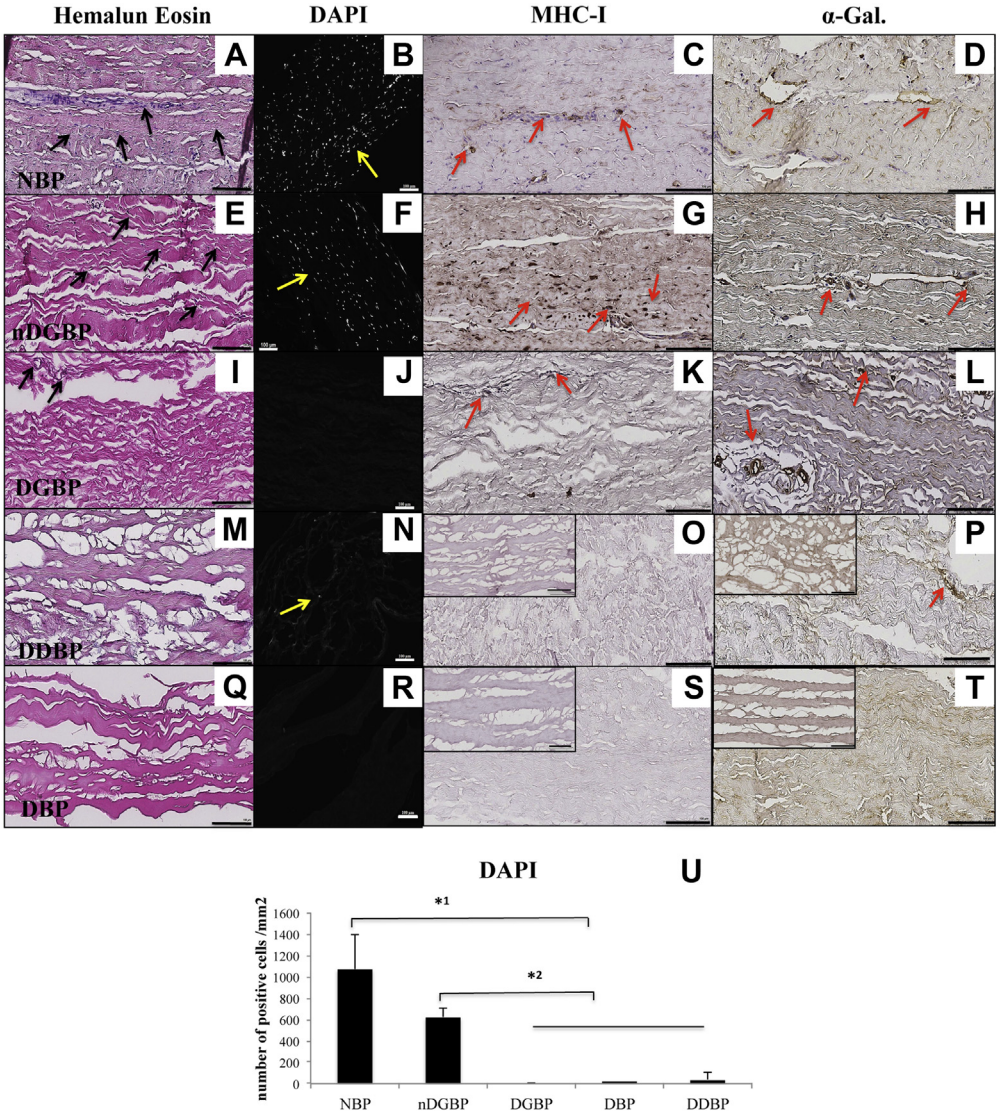

Fig. 1 – Histologic characterization of the NBP, nDGBP, DGBP, DDBP, and DBP with hematoxylin eosin, DAPI, and major antigens: MHC-1 and M86 (α-Gal) immunostaining. (Magnification is 20x and scale bar represents 100 μm). Nondecellularized tissues, NBP (A, B, C, and D) and nDGBP (E, F, G, and H) showed nuclei on hematoxylin eosin (A–E/black arrows) and DAPI (B-F/yellow arrows) staining. Presence of MHC-1 and α-Gal in these tissues was confirmed respectively for NBP (C-D) and nDGBP (G-H) (red arrows). The Dapi staining for DGBP (J) did not detect nuclei but some nuclei were visible at the periphery of the tissue on hematoxylin eosin (black arrow in I) and MHC-1 and α-Gal were still detected (red arrows in K-L). Some traces of nuclear material were stained with DAPI for DDBP (yellow arrow in N) but not visible on hematoxylin eosin (M). In the images O, P, S, and T, the larger microphotography is the stained tissue before gamma irradiation (nongamma irradiated DBP–O, P, and DDBP–S, T). The smaller photo in the right angle shows DBP and DDBP. Some traces of α-Gal were still visible on DDBP before gamma irradiation (P), but no staining was on the final product–DDBP (small photo in the right angle–P). This phenomenon did not occur for MHC-1 staining (O), which was negative before and after gamma irradiation. Perfect decellularization (Q-R) and desantigenization (S-T) were seen for DBP. (U): DAPI cells count par mm square for NBP, nDGBP, DGBP, DDBP, and DBP. *1NBP vs DGBP, DBP, and DDBP with $P < 0.05$. *2nDGBP vs DGBP, DDBP, and DBP with $P < 0.05$.

Antigen removal

MHC class I staining was negative for DBP, DDBP, and slightly positive for DGBP (Fig. 1C, G, K, O, and S). The staining of the α-Gal was positive for nondecellularized tissues and DGBP, wheras the staining for DBP and DDBP was negative (Fig. 1D, H, L, P, and T).

DNA

DNA quantification indicated lower decellularization of DDBP in comparison with DBP and significant reduction in DBP in comparison with NBP ($P < 0.05$; Fig. 2A). DNA detection on nDGBP and DGBP was low, but the tissues were not well digested despite doubling the dose of proteinase K and crushing these tissues.

Scanning electron microscopy

SEM showed decellularization of DGBP, DDBP, and DBP, but ruptures of collagen fibers were evidenced for gamma-irradiated tissues (DBP and DDBP) (Fig. 2B).

Mechanical properties

Mechanical properties of the different prosthesis (stiffness and max load before rupture) were not altered in comparison with native pericardium ($P > 0.05$). The stiffness of nDGBP was, however, significantly higher than for the other treated tissues (24.70 ± 6.64 vs 14.37 ± 4.6 vs 12.45 ± 3.3 vs 11.15 ± 4.9 vs 13.63 ± 5.34 for nDGBP vs DGBP, DBP, DDBP, and NBP, respectively; $P < 0.05$). The maximal load before rupture was similar for all treated tissues (Fig. 2C).

In vivo

Subcutaneous implantation

Immunogenic response

At 1 month, the anti-bovine antibody response was positive for all rodents receiving subcutaneous implants of NBP and for two rodents with DDBP. There was no anti-bovine or antibody production for other treated tissues.

After 4 months, low positive response was detected for one nDGBP and DGBP. Detection was still positive for all NBP and the two DDBP (Fig. 3A).

Tissue remodeling/cell incorporation, calcifications, and inflammatory reaction

The cellular recolonization was more homogeneous for DBP and impacted all layers (Fig. 3B).

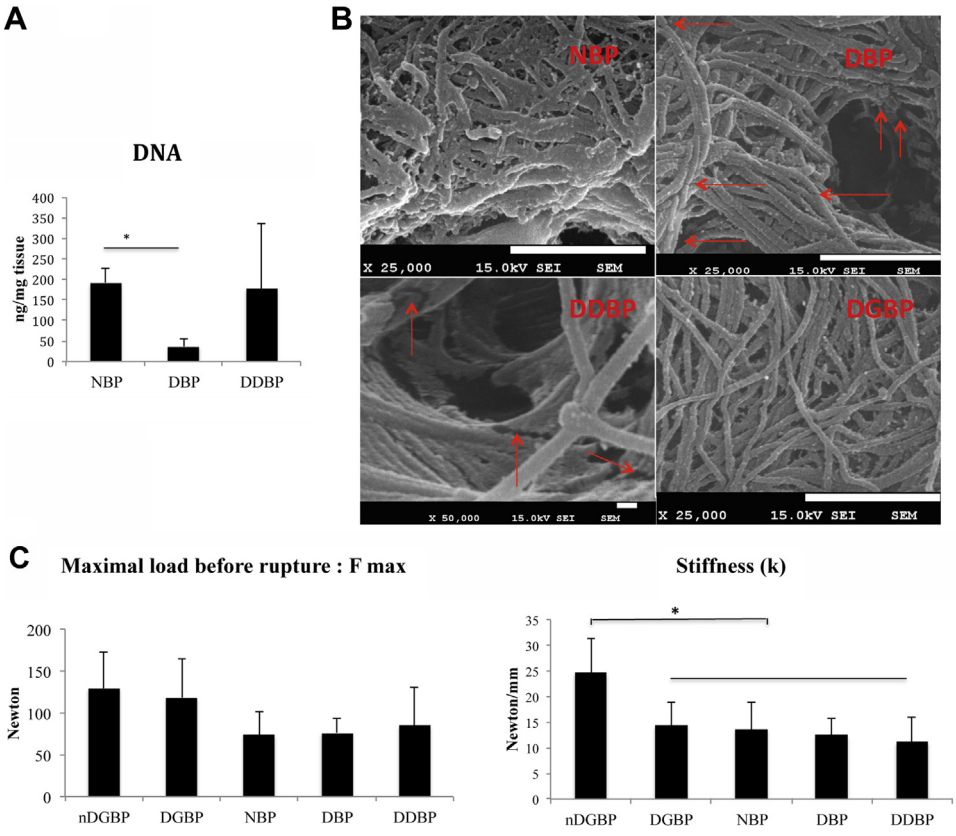

Fig. 2 – Characterization of the grafts: DNA content (A), SEM (B), and mechanical tests (C). (A) DNA content of NBP, DBP, and DDBP. DNA level was inferior to 50 ng/mg tissue for DBP but was higher for DDBP. *: DBP vs NBP with $P < 0.05$. (B) SEM of NBP, DBP, DDBP, and DGBP (scale bar 100 μm). The red arrows indicate collagen fibers rupture. (C) Mechanical tests showed no alteration of mechanical tissues properties after treatments. No significant differences were detected between tissues regarding maximal load before rupture. However, the nDGBP tissue showed significantly higher stiffness than other tissues. (*: nDGBP vs DGBP, NBP, DBP, and DDBP with $P < 0.05$).

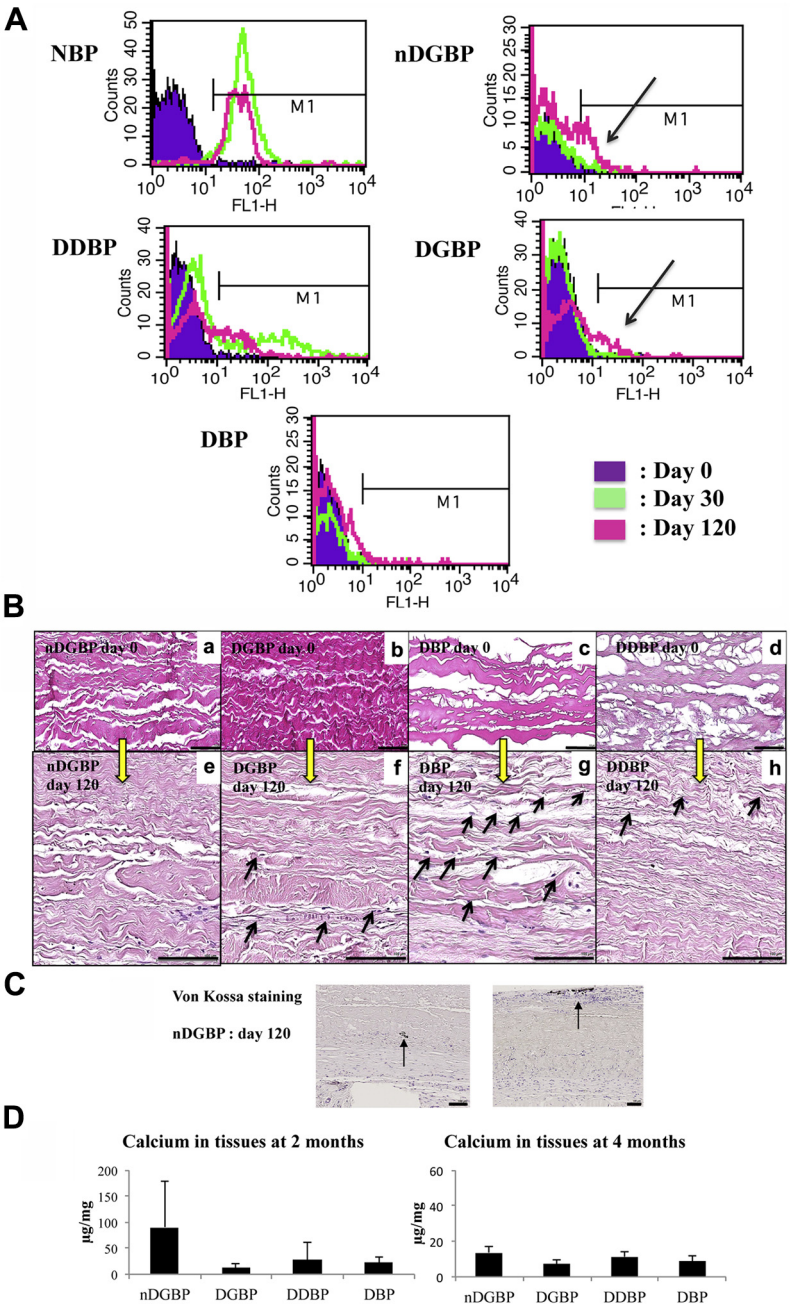

Fig. 3 – Results of the subcutaneous tests for (A) immunization test, (B) implants remodeling at 4 months, (C) von Kossa staining at 4 months, and (D) calcium implants content after 4 months. (A) Panel A shows results of the FACS for the detection of specific antibodies to bovine protein in the sera of rodent before (day 0 in purple) and after (day 30 in green and day 120 in pink) subcutaneous implantation of NBP, nDGBP, DGBP, DDBP, and BDP tissues. No reactions were noted for DBP. Immunization at day 30 was detected for all rodent they received NBP and for half rodents with DDBP. Late immunization, at day 120, was detected for 1 nDGBP and 1 DGBP (as indicated by black arrows). (B) Illustration of the recellularization after 4 months of nDGBP (a, e), DGBP (b, f), DBP (c, g), and DDBP (d, h) implanted in subcutaneous position with hematoxylin eosin staining. The original magnification is 20×, and scale bar represents 100 μm. Histology of tissues before implantation is on a, b, c, and d and after explantation at 4 months follow-up on e, f, g, and h. The black arrows in f, g, and h indicate nuclei and cell colonization. The recellularization process goes deeper in the DBP tissue (g). (C) Images of the positive von Kossa staining at 4 months in the subcutaneous model of nDGBP patches (scale bar 100 μm). The black arrow indicates the positive staining. (D) Subcutaneous implanted tissues calcium quantification after 2 months and 4 months follow-up. No significant difference between tissues was detected (P = NS).

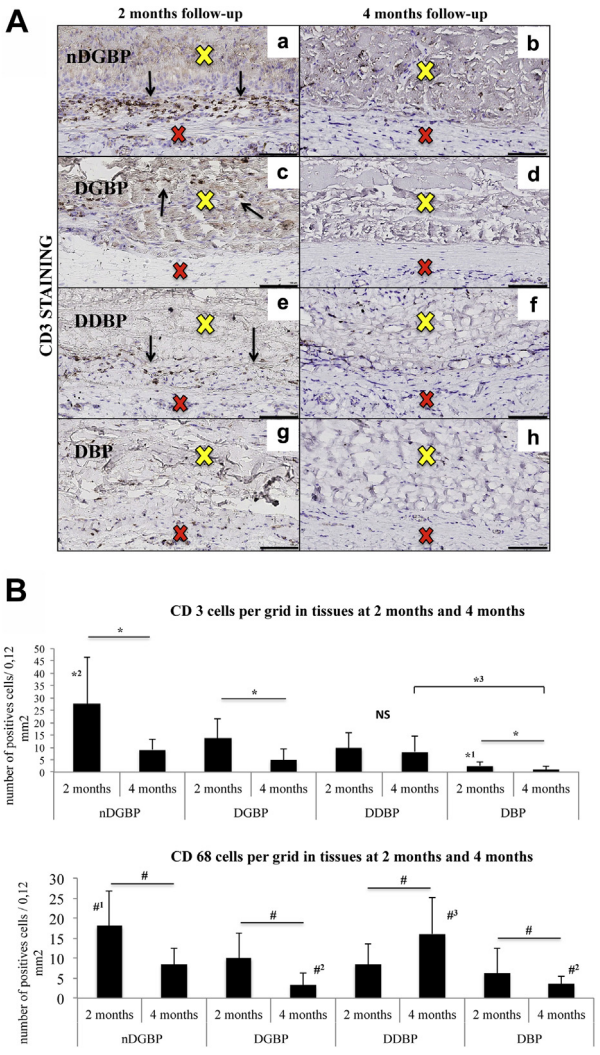

Fig. 4 – Biocompatibility/local inflammatory reaction assessment of subcutaneous implants (nDGBP, DGBP, DDBP, and BDP) with CD3 and CD68 immunostaining (A) CD3 immunostaining at 2 and 4 months and (B) CD3 and CD68 cell counting at 2 and 4 months. (A) Microphotographs at 20x magnification of CD3 immunostaining of explanted tissues at 2 and 4 months, respectively, for nDGBP: (a, b); for DGBP: (c, d); for DDBP: (e, f); and for DBP: (g, h). The scale bar represents 100 μm. The black arrows show positive cells for CD3. The yellow cross indicates the implanted tissue. The red cross shows the host tissue. (B) Histomorphometry/cell counting for CD3 and CD68 immunostaining at 2 and 4 months. At 2 months, the CD3 reaction was significantly the lowest with DBP (*1) and the highest with nDGBP (*2) with $P < 0.05$. At 4 months, the reaction significantly decreased for all tissues (* with $P < 0.05$) except for DDBP ($P = NS$) and was not significantly different between DBP and DDBP (*3 $P = NS$). The macrophagic reaction followed the same kinetic with significant intensity reduction after 4 months for all tissues except for DDBP, which showed significant inflammation increase (# with $P < 0.05$). However, at 2 months, the CD68 reaction was similar with DBP, DGBP, and DDBP and significantly lower than with nDGBP (#[1] with $P < 0.05$). At 4 months, the nDGBP leads to significantly greater reaction than DGBP and DBP (#[2] with $P < 0.05$). The highest macrophagic reaction was related to DDBP in comparison to all tissues (#3 with $P < 0.05$).

Although some calcium deposit could be observed in the nDGBP (von Kossa staining; Fig. 3C), the calcium quantification did not show any difference between the groups (Fig. 3D).

The inflammatory reaction was predominantly localized around the implants although the infiltration remained significant in the DGBP tissues (Fig. 4A, C, E, and G).

The CD3 staining was significantly reduced between 2 and 4 months in all treated tissues except for DDBP, which remained similarly infiltrated by lymphocytes ($P < 0.05$; * in Fig. 4B).

At 2 months, the DBP led to the lowest CD3 infiltration ($P < 0.05$), whereas the nDGBP led to a significantly higher CD3 staining ($P < 0.05$; *1 and *2 in Fig. 4B).

At 4 months, significant lower CD3 infiltration was quantified with DBP than with nDGBP and DDBP, respectively (1.08 ± 1.07 cells/0.12 mm^2 vs 9.08 ± 4.38/8.24 ± 6.13 cells/0.12 mm^2 with $P < 0.05$) and lower than with DGBP but not significantly. The CD3 staining was similar between nDGBP, DGBP, and DDBP (*3 in Fig. 4B).

The macrophages (CD68) were localized essentially around the implants, and the infiltration was more important after 2 months in nDGBP group ($P < 0.05$) in comparison to other groups while there was no difference between other tissues (#[1] in Fig. 4B).

The CD68 staining was significantly reduced after 4 months for nDGBP, DGBP, and DBP ($P < 0.05$) but not with DDBP leading to significant higher infiltration (16.08 ± 1.91 vs 6.28 ± 6.1 cells/0.12 mm^2 with $P < 0.05$; # in Fig. 4B).

At 2 months, CD68 infiltration was more significant in the nDGBP group ($P < 0.05$) in comparison with other groups while there was no difference between other tissues (Fig. 4B: #[1]).

At 4 months, the CD68 reaction was similar with DBP and DGBP tissues and was significantly lower for these tissues in comparison with nDGBP and DDBP (3.56 ± 1.91 positive cells/0.12mm^2 for DBP and 3.28 ± 3.03 with DGBP vs 8.44 ± 3.98 with nDGBP and 16.08 ± 9.12 with DDBP with $P < 0.05$) (Fig. 4B: #[2]).

However, the CD68 reaction at 4 months was significantly the highest with DDBP in comparison with other tissues ($P < 0.05$; #[3] in Fig. 4B).

Vascular implantation

Implantation

DBP and DHP were the easiest to suture. Perfect hemostasis was concomitant to vessel unclamping for these two tissues, whereas it was delayed for DGBP (Fig. 5A:1).

Follow-up and macroscopic assessment

Three rodents in the group DGBP died before 4 months due to a ruptured pseudo aneurysm, and one additional animal in this group showed a similar pseudo aneurysm at 4 months. No complications occurred with DBP or DHP. At 4 months, DHP patches were similar to native aorta (Fig. 5A: 2).

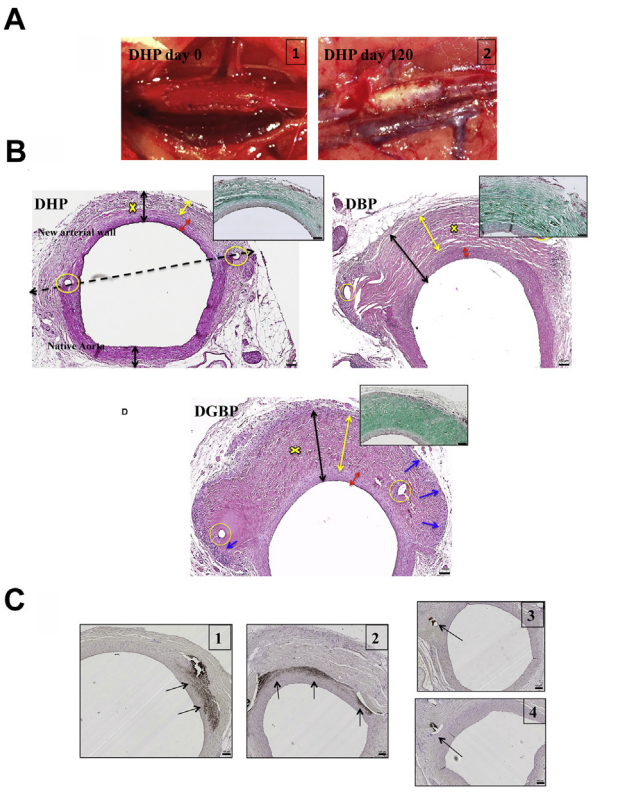

Fig. 5 – Vascular model: macroscopic view of DHP/tissues integration/tissues calcification. (A) The two images from left to right show (1) macroscopic view of implanted DHP on rodent abdominal aorta with running suture at day 0 and (2) macroscopic view of rodent patched abdominal aorta with DHP at 4 months. Note that a portion of the patch looks similar to the native artery. (B) Histology (hematoxylin eosin/Masson's trichrome-upper image) sample of patched abdominal aorta with DHP, DBP, and DGBP at 4 months (5x magnification/scale bar 100 μm) to illustrate patch integration. The interrupted black line shows the limit between the native vessel and the new artery wall/recellularized patch. Their respective thickness is indicated with the black arrows. The yellow cross indicates the implanted patch. The yellow arrow shows the thickness of the patch and the red arrow the new media thickness. The yellow circles surround the suture passage. (C) von Kossa staining: (1) positive staining in the reconstructed wall with DHP. (2) Positive staining in the reconstructed wall with DBP. (3) and (4) Positive staining of respectively DHP and DBP patches near the suture edge.

Tissue remodeling/cell incorporation, calcification, and inflammatory reaction

HE and Masson's trichrome staining showed evidence of patch recellularization with new vessels and cells in all decellularized matrices (Fig. 5B).

Von Kossa staining was positive between the matrix and the new intima/media for one DHP and one DBP (Fig. 5C: 1; 2). Some calcium deposits can also be visualized near the sutures in all groups (Fig. 5C: 3; 4).

The inflammatory reaction was essentially located in the external part of the reconstructed wall and near the sutures edges (Fig. 6A).

At 4 months, CD3 and CD68 infiltrations were significantly higher for DGBP compared to DBP and DHP, respectively, 65 ± 35.95 *versus* 7.28 ± 3.99 *versus* 6 ± 4.2 cells/0.12 mm^2 with $P < 0.05$ for CD3 (* in Fig. 6B) and 26.5 ± 13.87 vs 4.04 ± 2.09 vs 7.64 ± 4.64 cells/0.12 mm^2 with $P < 0.05$ for CD68 (* in Fig. 6C).

For the rodents that died before 4 months, with the commercialized DGBP patches, we observed intense inflammatory reaction and patch resorption near the suture.

Arterial wall regeneration

The recellularization was limited to the external part of the DGBP, deeper for the DBP patch and was complete for DHP patch (Fig. 7A, D, G, and J: A/D/G/J).

Acquisition of an arterial identity was confirmed by Miller, ASMA, and CD31 positive staining in all groups (Fig. 7A: B, E, H, K and Fig. 7A: C, F, I and L). At 4 months, important medial regeneration was observed in all groups, and the thickness was similar in all groups and similar to natives ($P < 0.05$; Fig. 7B).

The results of the study for the different products are summarized in a table (Fig. 8).

Discussion

The aim of this study is to determine *in vitro* and *in vivo*, in subcutaneous models, the biocompatibility of the bovine pericardium treated with a physical and chemical glutaraldehyde-free decellularization process (DBP) *versus* (1) the conventional detergent method (DDBP) *versus* (2) the Periguard method (DGBP), and (3) the Edwards non-decellularization and glutaraldehyde-based method considered as a standard (nDGBP). Then, an *in vivo* study, was conducted to compare, for arterial wall regeneration, the best bovine performing tissues of the subcutaneous study (DBP and DGBP) and the previously characterized human pericardium treated with the physical and chemical process (DHP).[11]

Tissue decellularization tries to overcome the limitations of current cardiovascular glutaraldehyde-fixed prosthesis[2,5,14] and homografts.[16,17] No standard process is well established.[13] Actually, following expert recommendations, different prosthesis assessment criteria were proposed to assess it before clinical use to avoid disastrous clinical results.[7,13,18,19]

Following these recommendations, this *in vitro* study showed that our processed BP (DBP) offers the best possibilities compared to other products. In contrast, the DDBP was not well decellularized unlike the study of Hulsmann despite using the same protocol.[14] In fact, despite long rinsing/washes, DDBP showed some detergent remnants at the surface that can also be at the root of lower biocompatibility.[20] Concerning DGBP, although having comparable surface properties to DBP, it showed in the depth some cells remnants and lower desantigenization. As for DGBP treatment, the DBP was also processed with NaOH 1 M for 1 hour. But as far as we know, on the basis of the commercial data, the preparation of

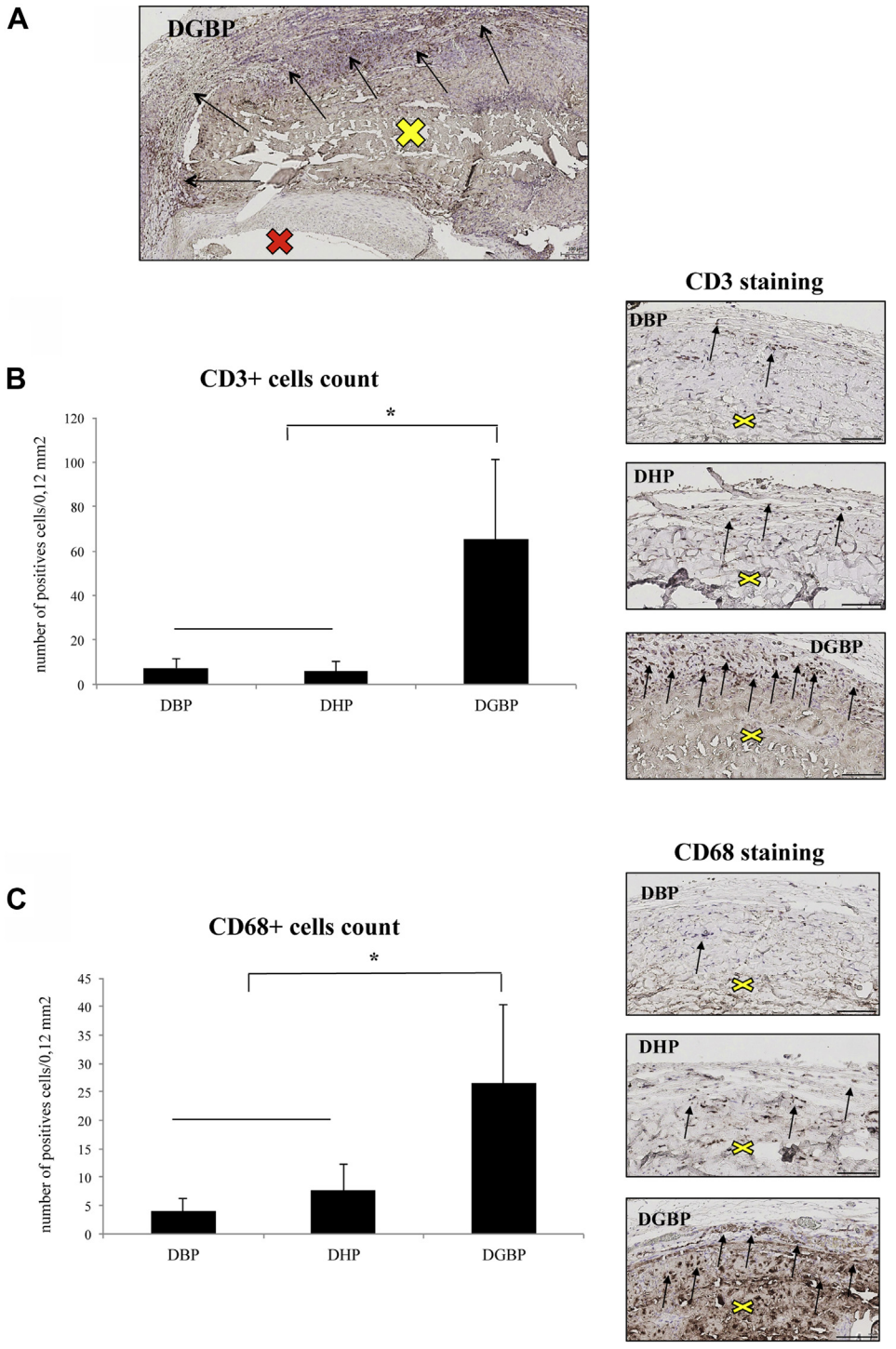

Fig. 6 – Biocompatibility assessment (CD3 and CD68 immunostaining) at 4 months with DBP, DHP, and DGBP implantation as vascular patch on the rodent abdominal aorta. (A)Histologic (CD3 staining/scale bar 100 μm) image of DGBP patch at 4 months illustrate inflammation is essentially located around the patch. The yellow cross indicates the patch, and red cross indicates the vessel lumen. (B) CD3 staining: the cell counting showed significant higher number of positive CD3 cells/0.12 mm^2 with the DGBP patch (*: DGBP vs DHP and DBP with $P < 0.05$). The histologic images (20x magnification/scale bar 100 μm) show the patch (yellow cross) surmounted by CD3 cells (black arrows) for the three different tissues. (C) CD68 staining: the cell counting showed significant higher number of positive CD68 cells/0.12 mm^2 with the DGBP patch (*: DGBP vs DHP and DBP with $P < 0.05$). The histologic images (20x magnification/scale bar 100 μm) show the patch (yellow cross) with CD68 cells (black arrows) at the periphery for the three different tissues.

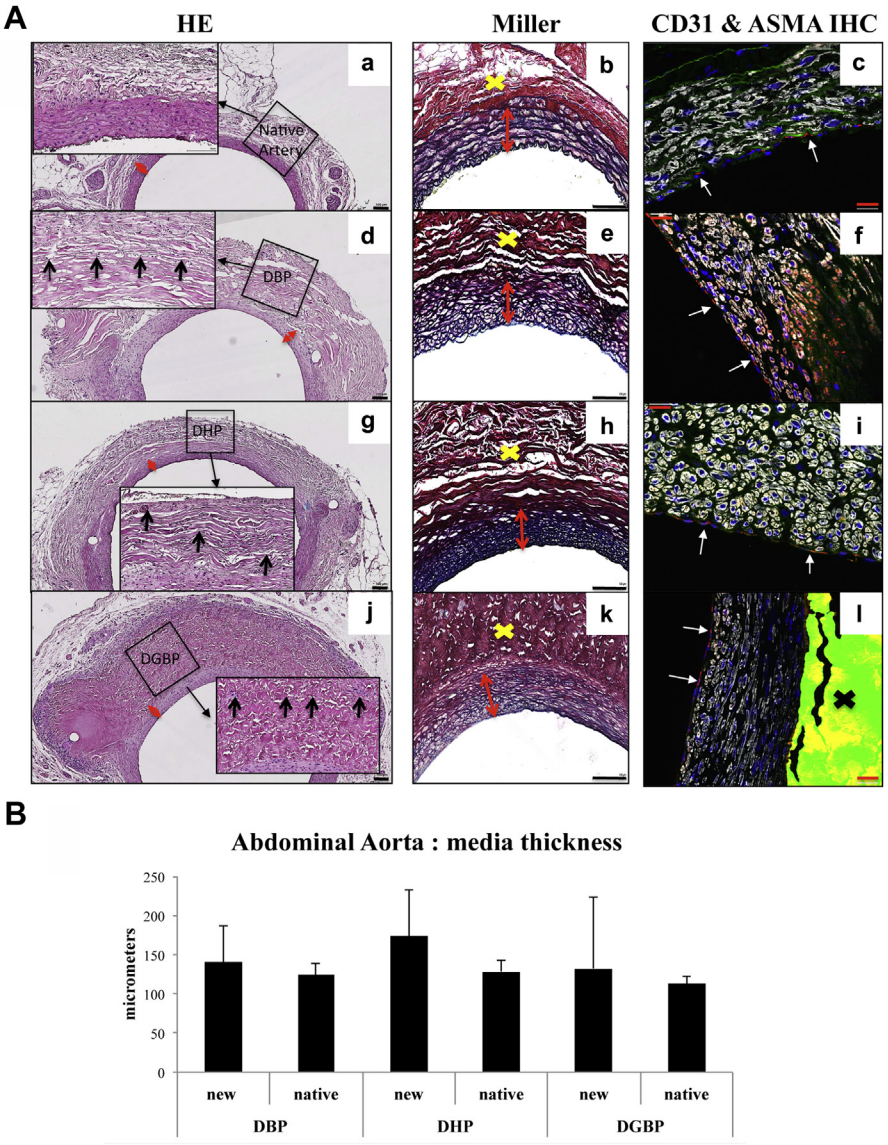

Fig. 7 – Assessment of arterial identity acquisition for the implanted DGBP, DBP, and DHP tissues in vascular position. (A) Native tissues are represented in a, b, and c; DBP tissues in d, e, and f; DHP tissues in g, h, and i; and DGBP in j, k, and l. The first column on the left (images a, d, g, and j): Hematoxylin eosin staining shows the patched aorta for each tissue and shows the recellularization of each tissue (5× magnification/scale bar 100 μm). The added image is the magnification of a patch area at the location indicated by the black rectangle. The black arrow indicates nuclei. The recellularization goes deeper for DHP group. The second column (images b, e, h, and k): Miller staining shows elastic fibers in the new media for each tissue. (20× magnification/scale bar 100 μm). The red double arrows delimit the thickness of the new media. The third column (images c, f, i, and l): CD 31 and ASMA immunofluorescent staining (CD31 and ASMA IHC) illustrates endothelialization of the patches (white arrows show red staining of endothelial cells) with a new media with smooth muscle cells stained in white (20× magnification/scale bar 100 μm). The black cross in the image l indicates the patch (DGBP). (B) The thickness of the new media is similar to native for each tissue and there is no significant difference between the tissues (P = NS).

DGBP is not associated with similar chemical agents that we used except ethanol for sterilization. In our protocol, however, ethanol recognized to reduce phospholipid content and known to play a role in calcification, is one step during the entire process and owing to some repeated washes,[3] the cytotoxicity of ethanol is eliminated. In addition, our process involved gamma irradiation, which is also recognized as a decellularization agent.[21]

After 1 month, study of *in vivo* immune reaction against bovine protein did not show differences between DBP and DGBP. More surprisingly, anti-bovine immunization was not evidenced with the nDGBP, whereas it is not at all decellularized. After 4 months however, and unlike DBP, DGBP and nDGBP evidenced an antibody response in one case. Some authors suggested the possibilities of delayed immune recognition with glutaraldehyde cross-linking:

Prosthesis characterization : Study results

In Vitro	NBP	nDGBP	DGBP	DDBP	DBP
Decellularization	-	-	+/-	+/-	+
Antigen removal	-	-	+/-	+/-	+
Mechanical integrity		+/-	+	+	+
In Vivo Subcutaneous		**nDGBP**	**DGBP**	**DDBP**	**DBP**
Remodeling		-	+/-	+/-	+
Low inflammation		-	+/-	-	+
No calcifications		+/-	+	+	+
In Vivo Vascular	**DHP**		**DGBP**		**DBP**
Post op.complications	-		+		-
Remodeling	+		+/-		+
Low inflammation	+		-		+
Arterial Identity	+		+/-		+

Fig. 8 – Tissue characteristics: study results. "+" signifies "yes" and "−" signifies "no".

glutaraldehyde should only avoid hyperacute or acute rejection.[13]

Regarding subcutaneous biocompatibility and local inflammation, at 2 months, our DBP offered the best results. Surprisingly, although nDGBP and DDBP were responsible of more inflammation, calcium quantifications were not different in comparison to DBP and DGBP tissues. However, our results are similar to a recent study of Griffith *et al.*, which showed no difference in terms of calcification between nondecellularized glutaraldehyde-fixed tissue and decellularized tissues in a subcutaneous model.[13] Similarly, we do not have a clear explanation of this phenomenon knowing that the subcutaneous model in the rodent is a recognized and widely used model for the evaluation of calcifications induced by cardiovascular prostheses.[22,23] The abdominal subcutaneous localization in comparison with the most commonly used dorsal subcutaneous location cannot explain this difference.[24]

After these *in vitro* and *in vivo* subcutaneous results, two tissues were retained as the best candidates for vascular regeneration: DBP and DGBP. In the vascular study, we intentionally chose a longer follow-up (4 months) than our previous study (1 month) to better assess vascular regeneration.[11]

The better prosthesis recellularization, which is of major concern for tissue regeneration, was achieved with DBP and DHP, whereas DGBP showed high periimplant inflammation. Furthermore, the results were marked with high mortality rate for DGBP. However, the mortality for this tissue was higher than in a similar study of Li *et al.*[25] In the group of DGBP, in early deaths, we observed intense inflammatory reaction near the suture edges. One explanation is that our suture line should be nearest/would be closer to the free edge of the patch than in the experiment done by Li *et al.*, in which they used interrupted sutures/simple stitches on smaller patches (3 mm per 1 mm). The inflammation should lead to tissue resorption and suture leakage creating pseudo aneurysm. However, this phenomenon did not occur with DBP and DHP. In addition, the FDA recently addressed a letter to healthcare providers relative to multiple adverse event reports as intraoperative or postoperative bleeding and hematomas associated with VascuGuard patch (Baxter International Inc) (a bovine pericardium treated with a similar process than PeriGuard [DGBP]) during carotid endarterectomy.[26] Considering these risks and the similarity with our results in the vascular model, our processed tissues are safer.

There are, however, some limits in our study. Experimentation on rodents does not allow us to implant large and long tissue segments as in clinical use. Preclinical models such as pigs or lambs will more accurately assess endothelialization and the risk of aneurysm formation of implanted tissues before clinical translation.[27]

Conclusion

In vitro, our combined physically and chemically processed bovine pericardium offers superior results in terms of decellularization than conventional detergent treated BP and the two commercially available BP. *In vivo*, in a subcutaneous model, our processed bovine pericardium (DBP) reached lower immunogenic and inflammatory responses than other bovine tissues. Eventually, in the intravascular rodent model, our human and bovine pericardia are less inflammatory than

Periguard pericardium and allow total arterial wall regeneration.

Acknowledgment

Authors' contributions: M.v.S., P.G., and T.S. contributed for study conception and design. Data acquisition was carried out by M.van.S., D.X., C.B., Y.G., J.D., and K.A. Analysis and data interpretation were carried out by M.van.S., P.G., T.S., D.X., and C.B. The authors M.van.S. and C.B. drafted the manuscript. P.G., D.X., C.B., and Y.G. critically revised the article.

The authors thank Marc Sinneave of the Institute of Mechanics, Materials and Civil Engineering, Materials and process engineering for mechanical tests assistance; Marie Henry, Rose-Marie Goebbels, Gwen Beaurin, and Martial Vergauwen for technical assistance; Pascale Segers and Eric Legrand for writing and administrative assistance; and Walter Hudders for figures layout assistance. The content of the work is solely the responsibility of the authors.

The authors received no specific grant from any funding agency in the public, commercial, or not-for-profit sectors.

Disclosure

The authors reported no proprietary or commercial interest in any product mentioned or concept discussed in this article.

REFERENCES

1. Ma B, Wang X, Wu C, Chang J. Crosslinking strategies for preparation of extracellular matrix-derived cardiovascular scaffolds. *Regen Biomater*. 2014;1:81–89.
2. Umashankar PR, Mohanan PV, Kumari TV. Glutaraldehyde treatment elicits toxic response compared to decellularization in bovine pericardium. *Toxicol Int*. 2012;19:51–58.
3. Choi JW, Kim DJ, Kim DJ, et al. Early results of novel bovine pericardial patch using Comprehensive Anticalcification Procedure in a Swine model. *ASAIO J*. 2016;62:100–105.
4. Manji RA, Zhu LF, Nijjar NK, et al. Glutaraldehyde-fixed bioprosthetic heart valve conduits calcify and fail from xenograft rejection. *Circulation*. 2006;114:318–327.
5. Vinci MC, Tessitore G, Castiglioni L, et al. Mechanical compliance and immunological compatibility of fixative-free decellularized/cryopreserved human pericardium. *PLoS One*. 2013;8:e64769.
6. Keane TJ, Swinehart IT, Badylak SF. Methods of tissue decellularization used for preparation of biologic scaffolds and in vivo relevance. *Methods*. 2015;84:25–34.
7. Simon P, Kasimir MT, Seebacher G, et al. Early failure of the tissue engineered porcine heart valve SYNERGRAFT in pediatric patients. *Eur J Cardiothorac Surg*. 2003;23:1002–1006.
8. Hopkins RA, Lofland GK, Marshall J, et al. Pulmonary arterioplasty with decellularized allogeneic patches. *Ann Thorac Surg*. 2014;97:1407–1412.
9. Neethling WM, Strange G, Firth L, Smit FE. Evaluation of a tissue-engineered bovine pericardial patch in paediatric patients with congenital cardiac anomalies: initial experience with the ADAPT-treated CardioCel(R) patch. *Interact Cardiovasc Thorac Surg*. 2013;17:698–702.
10. Mirsadraee S, Wilcox HE, Watterson KG, et al. Biocompatibility of acellular human pericardium. *J Surg Res*. 2007;143:407–414.
11. van Steenberghe M, Schubert T, Guiot Y, Bouzin C, Bollen X, Gianello P. Enhanced vascular biocompatibility of decellularized xeno-/allogeneic matrices in a rodent model. *Cell Tissue Bank*. 2017;18:249–262.
12. Wong ML, Griffiths LG. Immunogenicity in xenogeneic scaffold generation: antigen removal vs. decellularization. *Acta Biomater*. 2014;10:1806–1816.
13. Wong ML, Wong JL, Vapniarsky N, Griffiths LG. In vivo xenogeneic scaffold fate is determined by residual antigenicity and extracellular matrix preservation. *Biomaterials*. 2016;92:1–12.
14. Hulsmann J, Grun K, El Amouri S, et al. Transplantation material bovine pericardium: biomechanical and immunogenic characteristics after decellularization vs. glutaraldehyde-fixing. *Xenotransplantation*. 2012;19:286–297.
15. Steitz SA, Speer MY, McKee MD, et al. Osteopontin inhibits mineral deposition and promotes regression of ectopic calcification. *Am J Pathol*. 2002;161:2035–2046.
16. Carpentier A, Lemaigre G, Robert L, Carpentier S, Dubost C. Biological factors affecting long-term results of valvular heterografts. *J Thorac Cardiovasc Surg*. 1969;58:467–483.
17. Rajani B, Mee RB, Ratliff NB. Evidence for rejection of homograft cardiac valves in infants. *J Thorac Cardiovasc Surg*. 1998;115:111–117.
18. Cissell DD, Hu JC, Griffiths LG, Athanasiou KA. Antigen removal for the production of biomechanically functional, xenogeneic tissue grafts. *J Biomech*. 2014;47:1987–1996.
19. Voges I, Brasen JH, Entenmann A, et al. Adverse results of a decellularized tissue-engineered pulmonary valve in humans assessed with magnetic resonance imaging. *Eur J Cardiothorac Surg*. 2013;44:e272–e279.
20. Triglia D, Braa SS, Yonan C, Naughton GK. In vitro toxicity of various classes of test agents using the neutral red assay on a human three-dimensional physiologic skin model. *In Vitro Cell Dev Biol*. 1991;27A:239–244.
21. Crapo PM, Gilbert TW, Badylak SF. An overview of tissue and whole organ decellularization processes. *Biomaterials*. 2011;32:3233–3243.
22. Mako WJ, Vesely I. In vivo and in vitro models of calcification in porcine aortic valve cusps. *J Heart Valve Dis*. 1997;6:316–323.
23. Neethling W, Brizard C, Firth L, Glancy R. Biostability, durability and calcification of cryopreserved human pericardium after rapid glutaraldehyde-stabilization versus multistep ADAPT(R) treatment in a subcutaneous rat model. *Eur J Cardiothorac Surg*. 2014;45:e110–e117.
24. Mako WJ, Shah A, Vesely I. Mineralization of glutaraldehyde-fixed porcine aortic valve cusps in the subcutaneous rat model: analysis of variations in implant site and cuspal quadrants. *J Biomed Mater Res*. 1999;45:209–213.
25. Li X, Jadlowiec C, Guo Y, et al. Pericardial patch angioplasty heals via an Ephrin-B2 and CD34 positive cell mediated mechanism. *PLoS One*. 2012;7:e38844.
26. Maisel W. *Potential risk of Severe bleeding and hematomas associated with VASCU-GUARD peripheral vascular patch – letter to health care providers*; 2016. Available at: https://www.fda.gov/MedicalDevices/ResourcesforYou/HealthCareProviders/ucm518804.htm. Accessed September 1, 2016.
27. Byrom MJ, Bannon PG, White GH, Ng MK. Animal models for the assessment of novel vascular conduits. *J Vasc Surg*. 2010;52:176–195.